Available online at www.sciencedirect.com

ScienceDirect

Energy Procedia 160 (2019) 597–605

Energy Procedia

www.elsevier.com/locate/procedia

2nd International Conference on Energy and Power, ICEP2018, 13–15 December 2018,
Sydney, Australia

A thermo-hydraulic characteristics investigation in corrugated plate heat exchanger

Salman Al zahrani[a,b], Mohammad S. Islam[a], Suvash C. Saha[a*]

[a]School of Mechanical and Mechatronic Engineering, Faculty of Engineering and Information Technology, University of Technology Sydney, Ultimo NSW 2007, Australia
[b]Mechanical Engineering Department, Faculty of Engineering, Al Baha University, Saudi Arabia

Abstract

The amount of heat transfer from plate heat exchanger (PHE) is much higher compared with other types of conventional heat exchangers due to the high surface area of each plate. This study aims to investigate the heat transfer characteristics in a commercial corrugated PHE for sinusoidal corrugation type. A computational fluid dynamics (CFD) has been used to simulate the fluid flow inside the PHE for 1-1 single (water-water) and two (air-water) phase flow, counter arrangement. An advanced meshing technique has been used to generate the mesh for the PHE and a proper grid refinement test has been performed for the generated mesh. The overall investigation has been conducted for 60°/60° chevron angle plate (β) for a wide range of Re ($500 \leq Re \leq 3000$) and Prandtl number (Pr) ($0.72 \leq Pr \leq 7.5$). The result is validated with the benchmark experimental data. The impact of Reynolds and Pr has been investigated. The CFD results illustrate that the Nusselt number (Nu) increases with increasing of Reynolds number, while f decreasing with increasing of Re. The effect of Pr on Nusselt number and isothermal friction factor is presented. The corresponding correlations of Nu and f are developed from the CFD results.

Keywords: Plate heat exchanger; Chevron angle, CFD; Corrugation; Thermo-hydraulic characteristics.

1. Introduction

Novel PHE comprises of different number of plates; each one is opposite by 180° with respect to the adjacent plate. Consequently, a very small 3D channel (cross-corrugated passage) is generated between every two consecutive plates.

* Suvash C. Saha. Tel.: 61 2 9514 3183; fax: +61 2 9514 1530
E-mail address: suvash.saha@uts.edu.au

1876-6102
10.1016/j.egypro.2019.02.211

These plates have corrugations on their surfaces; the corrugations have their individual geometrical properties. Chevron angle is the most important one; it represents the inclination angle between the longitudinal centreline and the corrugation as shown in fig. 1. Also, there are other important parameters such as corrugation pitch, aspect ratio, and corrugation depth. Because of the existence of these parameters which can be varied according to the application requirement, it is quite hard to generate a heat transfer database for this kind of HEs. In spite of that, PHE is largely adopted due to their ability to work in places where temperature differences are very low along with the easiness of cleaning and the high heat transfer rate. They outspread in dairy, HVAC, petroleum companies, pharmaceutical industries, and many other applications.

One of the earliest efforts that studied the HTC of PHE was conducted by Troupe [1], which was carried out on plates of washboard type. After that several researchers [2-6] continued this investigation to expand the understanding of the thermal performance of this type of HEs. These studies were conducted on different types of plates, i.e., zig-zag, wavy-groove, and washboard type. In the last six decades starting with Emerson [7], the chevron plate type has become the popular one, and almost all researches on this field consider on this type of plates. One of the earliest contributions was provided by Okada [8]. The authors developed Nu and *f* correlations for different chevron angles, i.e., 15°, 30°, 45°, and 60°. The same study proved that the thermo-hydraulic performance of PHE is greater by 30% compared with the corresponding value of the conventional one. After that, different studies tried to incorporate the impact of different β and Re on Nu and f [9-12]. The main issue that makes the reader doubt is the discrepancy of their results for the same flow conditions. Therefore, there should be a systematic study that could identify the reason for these discrepancies. Among other factors, some researchers do not provide substantial information about their models [7, 13]. These make very hard to revisit their works to recognize the reason for the discrepancy of results.

Nomenclature			
		ΔP	Pressure drop, Pa
A	Effective heat transfer area, m^2	P_c	Corrugation pitch, m
$A_\circ$	Channel flow heat transfer area, m^2	t	Plate thickness, m
b	Corrugation depth, m	Greek	
C_p	Specific heat, $J/kg.k$	β	Chevron angle, °
d_e	Equivalent diameter, $d_e = 2b, m$	μ	Dynamic viscosity, $Pa.s$
f	Fanning friction factor	ρ	Fluid density, kg/m^3
G	Core mass velocity, $kg/m^2.s$	Subscripts	
h	Heat transfer coefficient, $W/m^2.k$	b	bulk fluid temperature
k	Thermal conductivity, $W/m.k$	c	Cold stream
L_h	Horizontal length from port to port, m	h	Hot stream
L_p	plate's channel effective length, m	i	Inlet condition
L_v	vertical length from port to port, m	m	Measured
L_w	flow channel width, m	o	Outlet condition
$\dot{m}$	Mass flow rate, kg/s	w	Wall
N	Number of channels		
Nu	Nusselt number		

It is quite hard to analyze the fluid flow and heat transfer inside PHEs experimentally. Therefore, numerical simulations have been utilized to provide a better understanding of the heat transfer mechanisms. Computational fluid dynamics (CFD) is one of the best tools that could simulate internal fluid flow and heat transfer such as in PHEs [14]. One of the earliest investigations that used CFD to study fluid flow inside PHE is conducted by Ciofalo [15]. On the other hand Kanaris et al., [16] performed a numerical study using two plates; one is corrugated, and the other is flat one. The corrugated plate was considered as the computational domain. The port

effect on both heat transfer and pressure drop was ignored. In fact, the existence of only one channel is not practical.
Also, it is not clear how the heat will be transferred in the existence of only one channel. In 2006, the same team [17] conducted another simulation study, however, this time three plates with β 60° were generated. The corrugations had a trapezoidal shape, which would definitely affect the flow and consequently affect the results. The port effect was ignored again. The heat transfer in the form of Nu for two symmetric PHEs with β 30°/30° and 60°/60° was investigated by Asif [13]. A details of the models were not provided i.e., the turbulence model, and the channel configurations were not provided. The Wilson plot technique was used to find the Re number exponent and the constant values in the Nu empirical equation. This long iterative process should be avoided, since CFD was used, which enables the user to find the temperature in any location on the model as well as the heat transfer coefficient value $'h'$ can easily be calculated.

The present PHE model has five plates, all with β 60°. It contains four channels; two of them belong to the cold side as utility channels, and the other two belong to the hot side as product channels. The port effect is considered in this study in an effort to simulate what is really occurring in real PHE.

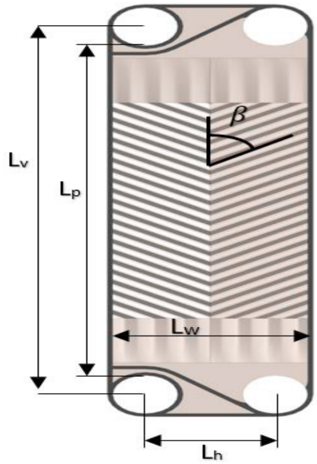

Fig. 1. Chevron plate type with its geometric parameters.

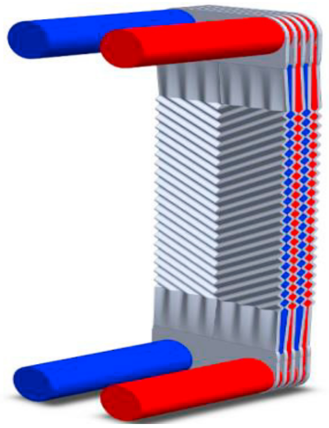

Fig. 2. Corrugated plate heat exchanger CAD model.

2. Model Setup

2.1. CAD Model Specifications

The PHE for β 60°/60° was generated by using Solidworks CAD 2016. The corrugations that formed on the plate surfaces are important to be created with the exact right dimensions i.e., the depth, the pitch and the roundness of the corrugation. In this model, all aspects of the real PHE were considered through the drawing process, including all points mentioned above, to get closer to the real PHE. The ports of both hot and cold channels were taken into consideration. They were created and merged each one with its channel as shown in fig. 2.

2.2. Mesh generation

The mesh was created using ANSYS CFD fluent v.19. A number of trials were carried out in order to specify the best mesh with good quality as shown in table 1. Since the model contains a very narrow passages, a tetrahedral mesh was implemented to ensure a good mesh distribution in the narrowly curved conduits. The grid independent test was carried out to make sure the results are stable, and the grid has no impact on them. Based on the test the grid size of 14.8 million elements was adopted for the proposed model.

Table 1. Mesh dependency test for a various number of mesh elements versus the average outlet temperatures.

Number of elements (million)	Outlet cold average temperature (K)	Outlet hot average temperature (K)
8	293.6	308.4
11	293.9	308.8
14.8	293.9	308.8
32	293.8	308.8

2.3 Plate material specifications

Stainless steel was set as the material of the plates, which is the most commonly used material for PHEs. Moreover, it is cheaper compared with other materials i.e. aluminium, and it has good physical and chemical properties. In addition, stainless steel was used in the benchmark experimental study [10]. Therefore, the plates of the current model were made up of the same material in order to compare the results. Thermal conductivity for our material is 16.27 *W/m.k,* and density is 8030 kg/m^3.

3. Mathematical Formulation

The heat transfer data obtained for the current study was at steady state conditions, they were expressed in the form of non-dimensional parameters, Nusselt number is employed as a sign of the heat transfer improvement, and friction factor is f employed as a sign of isothermal pressure drop inside the hot side channels. The equivalent diameter 'd_e' was calculated as twice the corrugation depth $'2b'$,

$$Re = \frac{\dot{m}\, d_e}{\mu\, A_\circ N} \tag{1}$$

$$Q_h = \dot{m}_h c_{p,h}\left(T_{h,i} - T_{h,o}\right) = h_h A(T_{h,b} - T_{w,h}) \tag{2}$$

$$Q_c = \dot{m}_c c_{p,c}\left(T_{c,o} - T_{c,i}\right) = h_c A(T_{w,c} - T_{c,b}) \tag{3}$$

where $T_{h,b} = \frac{(T_{h,i}+T_{h,o})}{2}$, $and\ T_{c,b} = \frac{(T_{c,i}+T_{c,o})}{2}$. The energy balance for hot and cold sides was checked. Theoretically, the difference between two sides should be zero. The difference in the current study was always found to be very low < 1%, which indicates the accuracy of the results. Also, it is worthy to point out that, in fluent, the average hot side wall temperature could easily be found, which is a unique feature of CFD over experimental approach. Then;

$$h_h = \frac{Q}{A(T_{h,b} - T_{w,h})} \tag{4}$$

Now, the hot side Nusselt number is determined as:

$$Nu = \frac{h_h d_e}{k} \quad (5)$$

The entire pressure drop across the PHE is calculated as;

$$\Delta P_m = \Delta P_{port} + \Delta P_{core} + \Delta P_{elev.} \quad (6)$$

Based on the average port velocity, the port pressure drop was estimated according to the empirical correlation provided by [18-20];

$$\Delta P_{port} = 1.5(\frac{\rho V^2{}_{port}}{2}) \quad (7)$$

$\Delta P_{elev.}$ was ignored since the plate length is small.

$$\Delta P_{core} = \Delta P_m - \Delta P_{port} \quad (8)$$

Now, based on [21], the isothermal fanning friction factor was estimated as:

$$f = \frac{\rho d_e \Delta P_{core}}{2 L_P G^2} \quad (9)$$

Where G represents the core mass velocity, which is defined as:

$$G = \frac{m^{\cdot}}{L_w b N} \quad (10)$$

3.1 Turbulence model

To investigate the heat transfer characteristics inside PHE the realizable $\boldsymbol{k-\varepsilon}$ model with scalable wall function as near wall treatment was adopted. The $\boldsymbol{k-\varepsilon}$ model describes the turbulence effect by solving two transport equations, the turbulence kinetic energy $\boldsymbol{k}$, and its dissipation rate $\boldsymbol{\varepsilon}$. The assumption of isotropic turbulence viscosity is applied in this model [22]. Other turbulence models including $\boldsymbol{k-\omega}$, LES, RSM were tested. The obtained results were compared with those of $\boldsymbol{k-\varepsilon}$ model. The realizable $\boldsymbol{k-\varepsilon}$ model found to be the best model that provides with a consistent results, as well as matches with the experimental results.

3.2 Boundary Conditions

The inlet boundary condition was set as the velocity inlet. The fluid velocity was calculated according to the mass flow rate corresponding to the required Reynolds number. Then according to the port shape “circular” and diameter, the inlet velocity was calculated. The temperature of the same fluid was also specified along with the inlet velocity. Five percent turbulence intensity was found to be the suitable value for the current flow pattern according to the Fluent [23]. The outlet boundary conditions were specified as pressure outlet. The gauge pressure value was constant and equal zero in order to prevent the reverse flow. The working fluids were water-water and water-air. For all cases, water at 18°C was used on the cold side.

3.3 Validation of the model

The numerical model was carefully generated and simulated to be as close as possible to the real model. Thus, the results were compared with the experimental one conducted by Manglik [10] as shown in fig. 3.

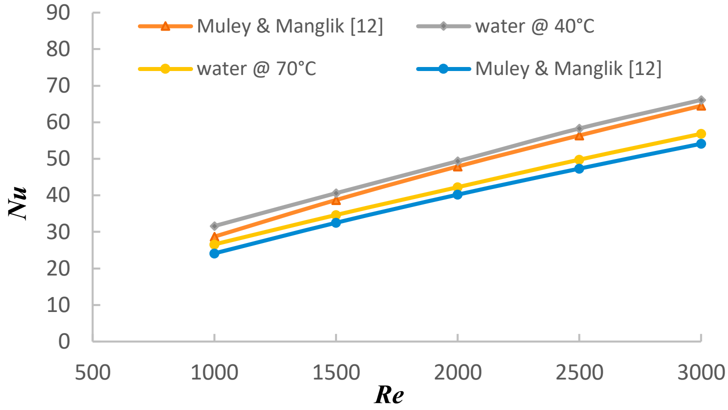

Fig. 3. Comparison between numerical and experimental Nu values with varying Re.

Note that, Manglik correlation was validated starting from Re ≥ 1000, the working fluid in that experiment was water. The maximum deviation was 10% for different inlet temperatures of 40°C and 70°C, which indicates good consistency between the numerical and the experimental results. Many factors could contribute the deviation such as different dimensions, i.e. corrugation wavelength, depth. Actually a small difference in corrugation roundness between the studies could cause a change in Nusselt number up to 18% as reported by [24]. However, the deviation is always ≤ 10% for all cases investigated in the current study.

4. Results and Discussion

The tests have been conducted for single phase (water-water) flow and two-phase (air-water) flow. The chevron angle β was considered as 60°/60°. Two sets of simulations were carried out; the first simulation was for hot air, and the second one was for hot water. The cold channel side has been kept as cold water for all cases. The Reynolds number varied from 500 to 3000. The results were expressed in the form of non-dimensional parameters, Nusselt number as a scale of heat transfer improvement, and isothermal fanning friction factor as a scale of pressure drop inside the channel. The calculations have been performed on the hot side of the PHE.

Figs. 4 (a, b) represent the hot air and hot water velocity contour at the middle channel of the PHE, respectively. The velocity distributions of the fluids for both cases are similar. The fluids velocity is not uniformly distributed through the channel. The corrugations of two consecutive plates are opposite to each other in order to promote the turbulence rate. This complexity may explain the non-uniformity of the fluids distribution. The dark blue points that distributed along the hot channel are stagnant points. These stagnation areas occurred due to the existence of contact points between the consecutive plates.

The temperature contours of hot air and hot water at the middle channel are shown in fig. 5 (a) and (b), respectively. In the case of the hot air, its temperature shows much faster-decreasing rate as air moves upward through the channel compared with hot water that subjected to the same conditions. This is because the heat diffusivity rate in case of air is higher than that in the case of water. In addition, air can absorb or lose heat by about more than four times compared with water, where its specific heat is much lesser than that of water.

For hot water and hot air, the Nusselt number increased as Reynolds number increases. Also, the increase in Nusselt number values was consistent. It was increased almost by 50% between each consecutive for Re = 500. When Re increased, the velocity also increased, which indicates that the rate of mass transfer increases simultaneously, and hence showed more convective heat transfer rate.

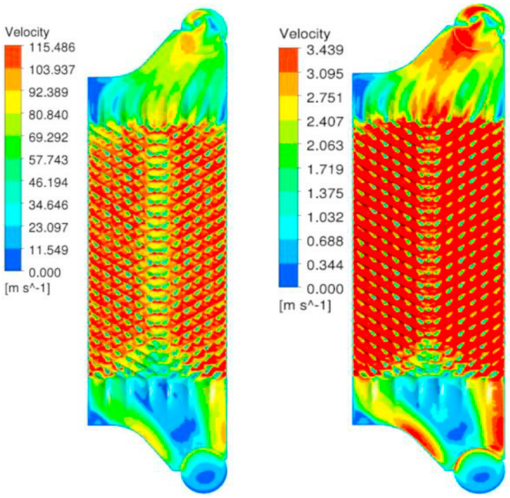

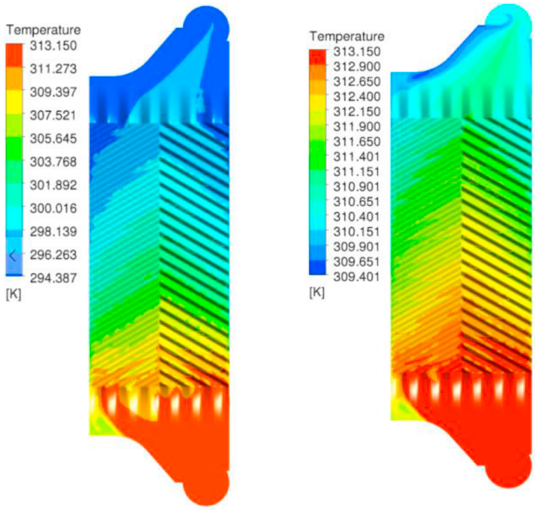

Fig.4 a) hot air velocity contour Re = 3000 b) hot water velocity contour Re = 3000 Fig. 5 a) hot air temperature contour Re = 3000 b) hot water temperature contour Re = 3000

For the first time, tests conducted on two different fluids (air and water) with the same conditions (PHE, channel number, and same physical conditions) to find out the impact of Prandtl number on the thermo-hydraulic performance in PHE. Both hot fluids inlet temperature was 40 °C $\left(Pr_{h,w} = 4.34, Pr_{h,air} = 0.72\right)$ whereas, the cold side inlet temperature was 18 °C for all cases. The Nu was significantly boosted simultaneously with Pr increasing about 2.5 to 4 times as shown in fig. 6. Since the Pr is the ratio between the viscous boundary layer thickness to the thermal one, Nu increases with higher Pr number. The thickness of thermal boundary layer is smaller in case of higher Pr number, consequently less thermal resistance by that boundary layer.

On the other hand, the friction factor decreased as the Re number increases in all cases, which is consistent with other studies [8, 25-27]. Although, the increase in Pr enhances the heat transfer, it causes an increase of friction factor inside the channel, which is due to the greater viscous boundary layer especially at low Re. When Re> 1500, the change in friction factor values was insignificant as shown in fig. 7.

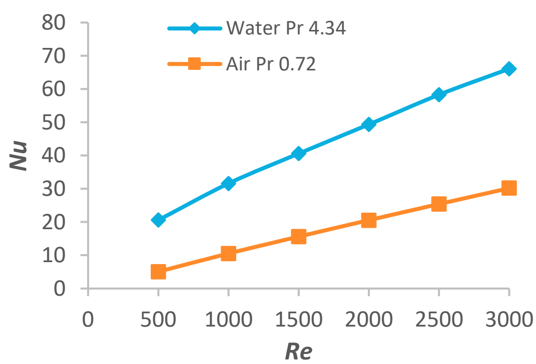

Fig. 6. Nu versus different Pr and Re values

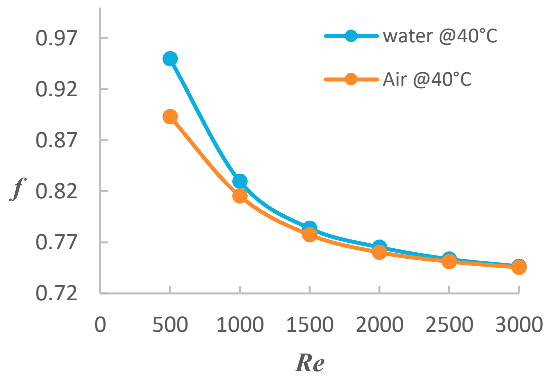

Fig. 7. Friction factor for different Pr versus varying Re values

4.1 Nu and f correlations

New correlations for both Nu and *f* were generated for β 60°/60°, $500 \leq Re \leq 3000$, and $0.72 \leq Pr \leq 7.5$. For *Nu* the classical Sieder [28] empirical correlation (11) was applied. The values of constant *C* and exponent *p* was found by applying the regression analysis technique over the range of Re. The Pr exponent value "n" were investigated over a range of different Pr and 1/3 found to give the best approximation.

$$Nu = CRe^{p}Pr^{n}\left(\frac{\mu}{\mu_w}\right)^{0.14} \quad (11)$$

For hot water $\beta = 60°/60°$

$$Nu = 0.238Re^{0.6417}Pr^{1/3}\left(\frac{\mu}{\mu_w}\right)^{0.14} \quad (12)$$

For hot air $\beta = 60°/60°$

$$Nu = 0.011175Re^{1.0025}Pr^{1/3}\left(\frac{\mu}{\mu_w}\right)^{0.14} \quad (13)$$

For isothermal fanning friction factor *f*, the Kumar [29] empirical equation (14) was applied, the correlations are as following in equations (15) & (16).

$$f = CRe^{m} \quad (14)$$

For hot water $\beta = 60°/60°$

$$f = 2.15\ Re^{-0.1342} \quad (15)$$

For hot air $\beta = 60°/60°$

$$f = 1.67\ Re^{-0.1023} \quad (16)$$

5. Conclusions

Thermo-hydraulic performance of commercial corrugated PHE was numerically investigated for two different hot fluids (air and water). The cold channel always kept as cold water. Tests of different CFD turbulent models were carried out. A realizable $k - \varepsilon$ model with scalable wall function as near wall treatment proved to give the most accurate and consistent results. Re ranging from 500 to 3000, two Pr values of 0.72 for air and 7.5 for water were adopted. The simulations have been conducted on counter-current, 1-1 pass, and for β 60°/60° for all cases. The Nu values showed higher values for both higher Re and Pr for all simulations. The isothermal friction factor showed lower values with higher Re values, but higher with higher Pr values. Based on the results, a new Nu and *f* correlations for β 60°/60° were proposed including the impact of Re, Pr, and viscosity variation effect.

Acknowledgment

The research authors would like to thank the University of Technology Sydney for their financial & technical support.

References

[1] Troupe, R, Morgan, J, and Prifiti, J, "The plate heater versatile chemical engineering tool." *Chemical Engineering Progress*. 56(1) (1960): 124-128.
[2] Buonopane, R, Troupe, R, and Morgan, J, "Heat transfer design method for plate heat exchangers." *Chemical Engineering Progress*. 59(7) (1963): 57-61.
[3] Clark, D, "Plate heat exchanger design and development." *Brewer* (1976).
[4] Crozier, R, Booth, J, and Stewart, J, "Heat transfer in plate and frame heat exchangers." *Chemical Engineering Progress*. 60(8) (1964): 43-45.
[5] Leuliet, JC, Maingonnat, JF, and Lalande, M, "Écoulements et transferts de chaleur dans les échangeurs à plaques traitant des produits visqueux newtoniens et pseudoplastiques 1. Modélisation des variations du diamètre hydraulique." *The Canadian Journal of Chemical Engineering*. 68(2) (1990): 220-229.
[6] Rene, F, Leuliet, J, and Lalande, M, "Heat transfer to newtonian and non-newtonian food fluids in plate heat exchangers: Experimental and numerical approaches." *Food and Bioproducts Processing*. 69 (1991): 115-126.
[7] Emerson, W, "The thermal and hydrodynamic performance of a plate heat exchanger: Flat plates-an apv exchanger-a de lavel exchanger-a rosenblad exchanger." (1967): *National Engineering Laboratory*.
[8] Okada, K, Ono, M, Tomimura, T, Okuma, T, Konno, H, and Ohtani, S, "Design and heat transfer characteristics of new plate heat exchanger." *Heat Transfer Japanese Research*. 1(1) (1972): 90-95.
[9] Savostin, A and Tikhonov, A, "Investigation of characteristics of plate-type heating surfaces." *Thermal Engineering*. 17(9) (1970): 113-122.
[10] Muley, A and Manglik, R, "Experimental study of turbulent flow heat transfer and pressure drop in a plate heat exchanger with chevron plates." *Journal of heat transfer*. 121(1) (1999): 110-117.
[11] Tovazhnyanski, L, Kapustenko, P, and Tsibulnik, V, "Heat transfer and hydraulic resistance in channels of plate heat exchangers." *Energetika*. 9 (1980): 123-125.
[12] Wanniarachchi, A, Ratnam, U, Tilton, B, and Dutta-Roy, K, "Approximate correlations for chevron-type plate heat exchangers". 1995, American Society of Mechanical Engineers, New York, NY (United States).
[13] Asif, M, Aftab, H, Syed, H, Ali, M, and Muizz, P, "Simulation of corrugated plate heat exchanger for heat and flow analysis." *International Journal of Heat and Technology*. 35(1) (2017): 205-210.
[14] Huang, J, "Performance analysis of plate heat exchangers used as refrigerant evaporators". 2011.
[15] Ciofalo, M, Collins, M, and Stasiek, J, "Flow and heat transfer predictions in flow passages of air preheaters: Assessment of alternative modelling approaches." *Developments in Heat Transfer*. 1997 (1997): 169-225.
[16] Kanaris, A, Mouza, A, and Paras, S, "Flow and heat transfer in narrow channels with corrugated walls: A cfd code application." *Chemical Engineering Research and Design*. 83(5) (2005): 460-468.
[17] Kanaris, AG, Mouza, AA, and Paras, SV, "Flow and heat transfer prediction in a corrugated plate heat exchanger using a cfd code." *Chemical Engineering & Technology: Industrial Chemistry-Plant Equipment-Process Engineering-Biotechnology*. 29(8) (2006): 923-930.
[18] Kakaç, S, Shah, RK, and Aung, W, "Handbook of single-phase convective heat transfer." (1987).
[19] Kays, W, "Loss coefficients for abrupt changes in flow cross section." *Trans. ASME*. 72 (1950): 1067-1074.
[20] Kays, WM and London, AL, "Compact heat exchangers." (1984).
[21] Kakac, S, Liu, H, and Pramuanjaroenkij, A, "Heat exchangers: Selection, rating, and thermal design." (2002): *CRC press*.
[22] Launder, B and Spalding, D, "The numerical computation of turbulent flows. Computer methods in applied mechanics and energy, 3, 269–289". 1974.
[23] "Fluent 6.3 user manual, access date 13.11.2018 https://www.Sharcnet.Ca/software/fluent6/html/ug/main_pre.Htm".
[24] Sparrow, E and Hossfeld, L, "Effect of rounding of protruding edges on heat transfer and pressure drop in a duct." *International Journal of Heat and Mass Transfer*. 27(10) (1984): 1715-1723.
[25] Focke, W, Zachariades, J, and Olivier, I, "The effect of the corrugation inclination angle on the thermohydraulic performance of plate heat exchangers." *International Journal of Heat and Mass Transfer*. 28(8) (1985): 1469-1479.
[26] Khan, T, Khan, M, Chyu, M-C, and Ayub, Z, "Experimental investigation of single phase convective heat transfer coefficient in a corrugated plate heat exchanger for multiple plate configurations." *Applied Thermal Engineering*. 30(8-9) (2010): 1058-1065.
[27] Thonon, B, Vidil, R, and Marvillet, C, "Recent research and developments in plate heat exchangers." *Journal of Enhanced Heat Transfer*. 2(1-2) (1995).
[28] Sieder, EN and Tate, GE, "Heat transfer and pressure drop of liquids in tubes." *Industrial & Engineering Chemistry*. 28(12) (1936): 1429-1435.
[29] Kumar, H. "Evaporation in plate heat exchangers". in *AICHE Symposium Series*. American Institute Of Chemical Enginners. (1993).